Photochemistry and Photobiology, 20**, **: *–*

Photochemical Reaction Between 1,2-Naphthoquinone and Adenine in Binary Water-Acetonitrile Solutions

Qiaohui Zhou[1], Yaxiong Wei[1], Xiang Liu[1], Lin Chen[1], Xiaoguo Zhou[1,2]* and Shilin Liu[1,2]

[1]Hefei National Laboratory for Physical Sciences at the Microscale, Department of Chemical Physics, University of Science and Technology of China, Hefei, Anhui, China
[2]Synergetic Innovation Center of Quantum Information & Quantum Physics, University of Science and Technology of China, Hefei, Anhui, China

Received 10 February 2017, accepted 19 June 2017, DOI: 10.1111/php.12808

ABSTRACT

The photochemical reaction between 1,2-naphthoquinone (NQ) and adenine was investigated using nanosecond time-resolved laser flash photolysis. With photolysis at 355 nm, the lowest triplet state T_1 of NQ was produced via intersystem crossing from its singlet excited state. The triplet-triplet absorption of the state contributes three bands of transient spectra at 374, 596 and 650 nm, respectively, in pure acetonitrile and binary water-acetonitrile solutions. In the presence of adenine, the observation of $A^{\cdot+}$ (at 363 nm) and $NQ_{+}H^{\cdot}$ radical (at 343 and 485 nm) indicates a multistep mechanism of electron transfer process followed by a proton transfer between ^{3}NQ* and adenine. By fitting with the Stern-Volmer relationship, the quenching rate constant k_q of ^{3}NQ* by adenine in binary water-acetonitrile solutions (4/1, volume ratio, v/v) is determined as 1.66×10^9 M^{-1} s^{-1}. Additionally, no spectral evidence confirms the existence of electron transfer between ^{3}NQ* with thymine, cytosine and uracil.

INTRODUCTION

Electron transfer (ET) is one of the most common photochemical processes. Usually, it is initiated by an oxidation process in the presence of photosensitizers with photo-irradiation (1,2). As ET in double-stranded DNA can lead to genetic information error reading and damage (1–3), ET from DNA nucleobases to the excited photosensitizer has attracted extensive interest. The typical bases, adenine (A), thymine (T), cytosine (C), guanine (G) and uracil (U) are usually the primary targets of ET to the excited photosensitizers (4,5). The oxidation energies (E_{ox}) of the five bases follow a sequence: G < A < T < C < U (6), and generally lower E_{OX} suggests more favorable ET probability.

Quinones are ubiquitous micromolecule compounds, and their derivatives often act as the key intermediates of dyes or disinfectants in pesticide and traditional medicine. According to their various biological activities, quinones play important roles in aerobic respiration and energy-producing photosynthesis (7–9) and participate in transport of electrons in cell membrane as a high-efficient electron acceptor (10,11). Due to the high redox potentials, quinones are commonly used as the photosensitizer in many photochemical processes. Therefore, several experimental and theoretical investigations have been performed on the ET between bases and quinones in the past decades (3,12,13).

Typical chemical reaction processes between photo-excited quinones and nucleobases involve ET and hydrogen atom abstraction (HA) (14,15). The mechanisms of ET and HA were identified in the photochemical reaction between tetrachloroquinone (TCBQ) with T and U (16). A series of experimental investigations on the reactions between nucleobases and several quinones, for example, 2-methyl-1,4-naphthoquinone (MQ), 9,10-anthraquinone (AQ) and benzoquinones (BQ), were performed by Basu and coworkers (17–20). Radical pairs and radical cations produced in the ET and HA processes were observed in transient-state photolysis (18,21). Interestingly, the ET efficiency from A, C, T and U to MQ showed a consistent order with the E_{ox} value (20). However, the probability of ET from three pyrimidines to AQ did not follow the E_{ox} sequence. The similar phenomena were observed in the photochemical reaction of 1,8-dihydroxyanthraquinone (DHAQ) and nucleobases (20,22). Therefore, the substituent group on pyrimidine or purine has shown a significant effect on the ET efficiency, as well as the E_{ox} values.

It is well known that both $n\pi^*$ and $\pi\pi^*$ excitation are involved in photo-excitation of quinones. With photolysis, the ET and HA processes of *p*-quinones occur via the triplet state T_1 of $n\pi^*$ character (23,24). Compared to *p*-quinones, only a few photolysis of *o*-quinones, for example, NQ and 9,10-phenanthrenequinone (PQ), has been performed (25–27). The time-resolved ESR confirmed that the dominant character of the T_1 state could be changed from $\pi\pi^*$ in ethanol to $n\pi^*$ in nonpolar solvents due to the smaller energy difference between $^3n\pi^*$ and $^3\pi\pi^*$ states in these *o*-quinones (28).

To our knowledge, there is no experimental investigation on the photochemical reaction between NQ and bases, although both the reactants are common electron acceptor and donor, respectively. In the present work, the photochemical reaction dynamics of NQ and four bases, A, T, C and U, are studied with a method of nanosecond time-resolved laser flash photolysis at 355 nm. Transient absorption spectra are measured to identify the major intermediates and products. The influence of solvent polarity on the absorption spectra and the reaction rates is also checked from pure acetonitrile to binary water-acetonitrile solutions. Based on the observed ET and/or HA processes, the interaction mechanisms between ^{3}NQ* and the bases are clarified and compared

*Corresponding author email: xzhou@ustc.edu.cn (Xiaoguo Zhou)

with the E_{ox} sequence of bases. An additional discussion is performed on influence of the substituent group and/or steric hindrance of bases.

MATERIALS AND METHODS

Materials. 1,2-NQ (97%) and bases (>99%) were purchased from Sigma-Aldrich and Fluorochem Inc., respectively, and used without any purification. The solvents were acetonitrile of high-performance liquid chromatography (Spectrochem) and triply distilled deionized water. The typical concentration of NQ was 5×10^{-4} M and that of DNA bases was changed from 5×10^{-4} to 5×10^{-3} M in experiments. Due to too low solubility of bases in pure acetonitrile, binary water-acetonitrile solutions were utilized to dissolve both NQ and bases efficiently, and two typical volume ratios of CH_3CN/H_2O were chosen as 9/1 and 4/1 (v/v). The influence of solvent polarity on photochemical reactions between NQ and the bases was discussed by comparing the dynamic behaviors in pure acetonitrile and binary water-acetonitrile solutions (Scheme 1).

Equipment. The present experiments were performed using a homebuilt nanosecond laser flash photolysis system. The details have been introduced previously (22,29,30), and thus only a brief description is presented here. The pulsed excitation light source was the third harmonic (355 nm, pulse duration 8 ns, pulse energy <7 mJ $pulse^{-1}$) of a Q-Switched Nd:YAG laser (PRO-190, Spectra Physics, repetition rate of 10 Hz). A 500 W Xenon lamp was used as the analyzing light source. The pulsed laser and the analyzing light passed perpendicularly through a flow quartz cuvette with an optical path length of 10 mm. A monochromator equipped with a photomultiplier (CR131; Hamamatsu) was used to measure the transient absorption spectra. The spectral resolution of the system was less than 1 nm. The dynamic decay curve of intermediate was averaged by 512 laser shots and recorded with an oscilloscope (TDS3052B; Tektronix). All the solutions were deoxygenated by purging with high purity argon (99.99%) for about 30 min before measurements. The steady-state UV-Vis absorption spectra were recorded from 300 nm to 650 nm with a UV spectrophotometer (UV-3600; Shimadzu). All the present photochemical experiments were performed at ambient room temperature (25°C).

Computation. All density functional theory calculations were performed with the Gaussian-09 program package (31). The geometry of NQ in the ground electronic state was optimized at the CAM-B3LYP level with the 6-311 + +G* basis set (32), while that of NQ in the low-lying excited singlet and triplet states was obtained with the time-dependent B3LYP (TD-B3LYP) level of theory. The vertical and adiabatic excitation energies of NQ were calculated at the same level. The solvent effect was taken into account by applying the Polarizable Continuum Model (PCM).

RESULTS AND DISCUSSION

In the steady-state absorption spectra of NQ and adenine in different solvents (shown as Figure S1), only two bands were observed in a wavelength range of 300–650 nm. In pure acetonitrile, the lower energy band is located at 398 nm as the $S_1 \leftarrow S_0$ transition of NQ, and the higher one is the $S_2 \leftarrow S_0$ absorption at 338 nm. The optimized geometries of singlet and triplet NQ at S_0, S_1 and T_1 are calculated and shown in Fig. 1, as well as the representation of major molecular orbitals. Obviously, the C=O bond lengths of S_1 and T_1 states are elongated from the values in the ground state because of the excited antibonding orbital.

The calculated vertical and adiabatic excitation energies of the low-lying electronic states of NQ in pure acetonitrile are summarized in Table 1 and agree with the experimental data. No parameters can be accurately predicted and used in PCM model for the mixed solvents. Thus, we only compared the calculated energies of the excited states and the optimized structures in pure acetonitrile and water with those in gas phase (the data are not shown in Table 1). Although there are no direct calculations on the mixed solvents, the changes in the steady-state absorption spectra confirm the solvent effect in the expected sequence. It is well known that both $n\pi^*$ and $\pi\pi^*$ excitations are involved in the $S_1 \leftarrow S_0$ absorption with the different weights. With the solvent polarity increase, the $\pi\pi^*$ excitation is gradually stabilized as the lowest singlet state (33,34). Thus the contribution from the $\pi\pi^*$ transition is enhanced in the $S_1 \leftarrow S_0$ excitation, and the maximum absorption exhibits a slight redshift in Figure S1.

Transient absorption spectra of NQ in pure acetonitrile and binary water-acetonitrile solutions

Figure 2(a) shows the transient absorption spectra of NQ in pure acetonitrile at different delay times, with photolysis at 355 nm. The sharp drop at 355 nm is the scattering of the excitation laser. Three dominant absorption peaks are observed at 374, 596 and 650 nm, respectively. The bands are attributed to the triplet-triplet absorptions, because all of them are quenched drastically in the presence of the solvated oxygen (see Figure S2). As suggested in the previous experiment (35), the bands at ~370, 600 and 650 nm are assigned as the absorption of the triplet NQ. In addition, the similar transient absorption spectra are observed with photolysis at 450 nm (see Figure S3), although the Frank-Condon excitation of NQ at 355 nm partially involves the $S_2 \leftarrow S_0$ transition. It implies that the internal conversion (IC) from S_2 to S_1 is much faster than the other photochemical processes, which agrees with the recent conclusions in deactivation of the excited states of quinones (36,37).

The dynamic decay curves were recorded at 374, 596 and 650 nm, respectively. All of them have the similar time profiles (see Figure S4), and hence only the curve at 374 nm was plotted in Fig. 2(b). Interestingly, both the excitation energies of the lowest two triplet states, T_1 and T_2, are lower than those of S_1 state as shown by the present TD-DFT calculations. Thus, with photolysis at 355 nm, both the T_1 and the T_2 states could be

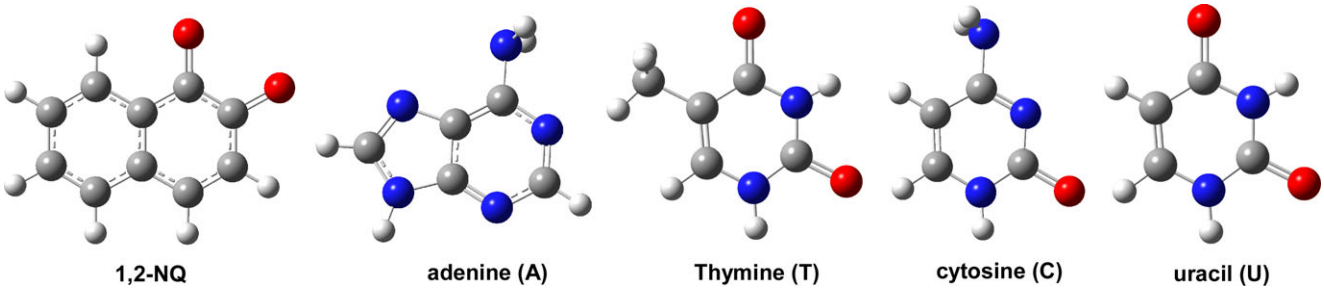

Scheme 1. Molecular geometries of 1,2-NQ and four bases.

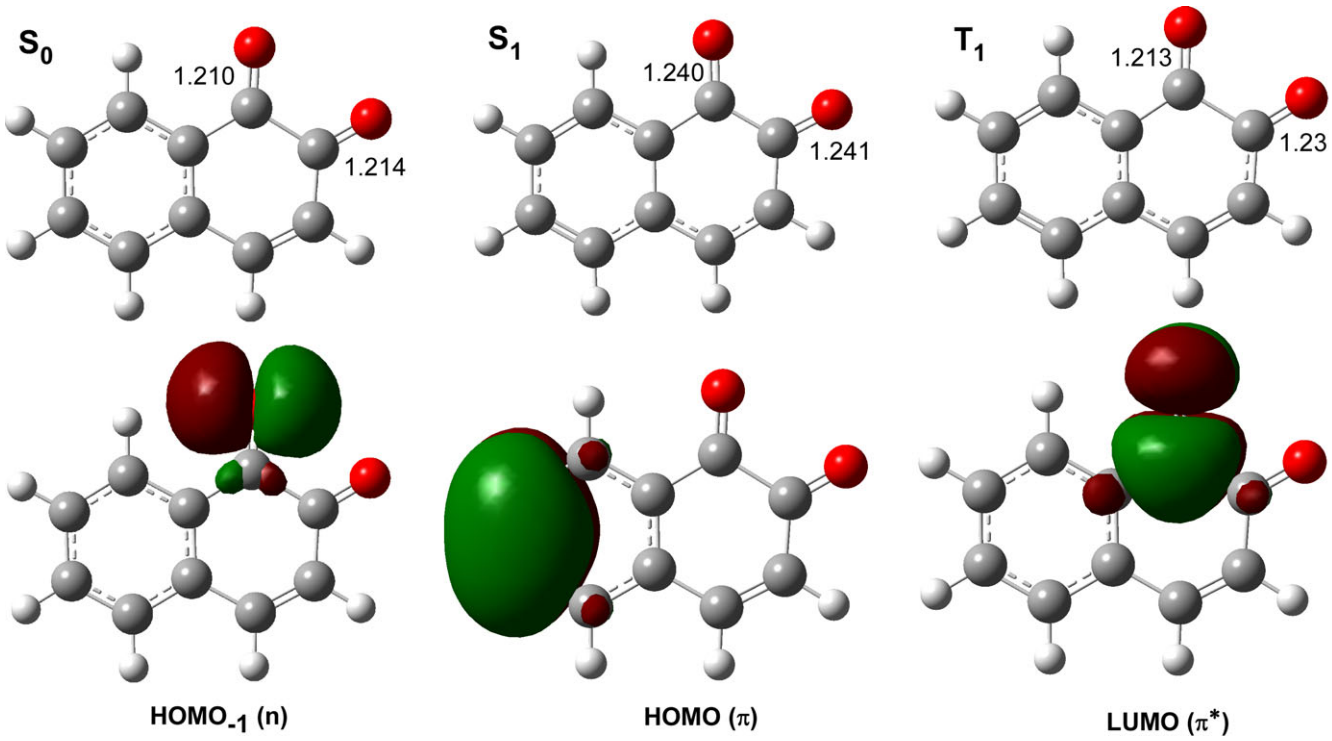

Figure 1. Optimized geometries of the ground, lowest singlet and triplet states of NQ, as well as the representation of major molecular orbitals.

Table 1. The calculated vertical and adiabatic excitation energies of NQ at CAM-B3LYP/6-311 + +G(d,p) level.*

	Vertical energy		λ /nm		Adiabatic energy			
	E/hartree	ΔE/eV	Cal.	Exp.	E/hartree	ΔE/eV	f †	Composition
S_1	−534.87817	3.08	403	398	−534.89228	2.69	0.1197	HOMO → LUMO
S_2	−534.84575	3.96	313	338	−534.85505	3.42	0.2149	$HOMO_{-1}$ → LUMO
T_1	−534.89383	2.65	468	–	−534.91372	2.11	0.0000	HOMO → LUMO
T_2	−534.88283	2.95	420	–	−534.89692	2.57	0.0000	$HOMO_{-1}$ → LUMO

*The energy of the ground electronic state of NQ is calculated as −534.99122 hartree. †Oscillator strengths.

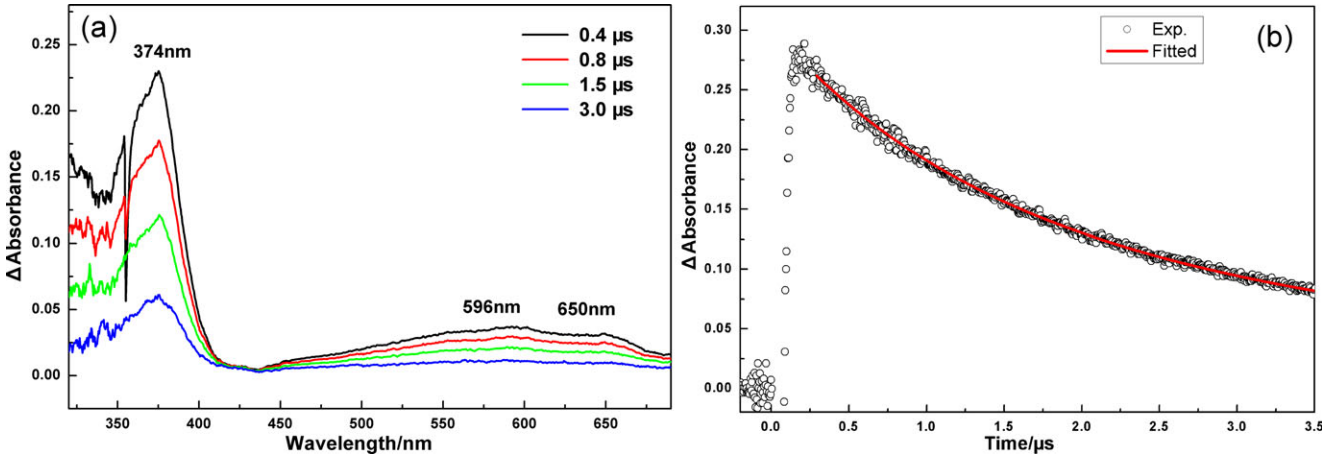

Figure 2. (a) Transient absorption spectra of NQ in pure acetonitrile at different delay times with photolysis at 355 nm. (b) Dynamic decay curve of the intermediate at 374 nm, where the fitted time profile is shown as well.

Table 2. Absorption wavelengths and quenching rates of various intermediates in solvents.

Band	I	II	III
NQ -CH_3CN			
λ(nm)	374	596	650
$k(\times 10^6\ s^{-1})$	8.19 ± 0.11	10.15 ± 0.20	9.96 ± 0.19
NQ -CH_3CN/H_2O 9/1			
λ(nm)	374	600	655
$k(\times 10^6\ s^{-1})$	7.52 ± 0.11	9.72 ± 0.18	9.57 ± 0.18
NQ -CH_3CN/H_2O 4/1			
λ(nm)	374	596	660
$k(\times 10^6\ s^{-1})$	7.04 ± 0.14	9.42 ± 0.15	9.60 ± 0.19

produced from ISC after the S_1 state is prepared. Because the fast internal conversion between T_2 and T_1 in aromatic compound is usually in picosecond timescale (36,38,39), we believe a similar decay rate for the internal conversion from T_2 to T_1 of NQ. Thus, the dynamic decay in Fig. 2(b) observed in experiment should be the photochemical behavior of ^{3}NQ* in the T_1 state.

The quenching rates of the intermediates in Fig. 2(a) can be obtained by fitting the decay time profile with a pseudo first-order kinetic. Table 2 summarizes the absorption wavelengths and the quenching rates of the intermediates. Acetonitrile as an inert solvent does not react with the triplet NQ, and thus the self-quenching by collision is most significant in the overall decay process. As shown in Table 2, the decay rates at 596 and 650 nm are close. The smaller value at 374 nm is thought due to influence of the nearby absorption band at the higher energy.

It is well known that the solvent polarity can affect the efficiencies of IC and ISC processes. The transient absorption spectra of NQ in two binary water-acetonitrile solutions were recorded and presented in Fig. 3. Neither significant shift nor change of intensity was observed with the three major triplet bands compared to those in Fig. 2(a). The decay rates of the three absorptions in binary water-acetonitrile solutions are summarized in Table 2 and similar to those in pure acetonitrile. The viscosities of the mixed solutions are increased with the fraction of water increase, which agrees with the slight decrease in the self-quenching rates at 374 nm in Table 2.

Additionally, two new weak and wide bands gradually appear at 343 and 420 nm, respectively, with the increased ratio of water. Harada *et al.* (35) assigned the absorption of the $NQ_{+H}^{\bullet}$ radical at 340 nm, and thus a HA process between ^{3}NQ* and water is expected in the present experiment to produce the $NQ_{+H}^{\bullet}$ radical. The further HA leads to formation of 1,2-dihydroxynaphthalene (NQ_{+2H}). As suggested by Kuhmet al. (40,41), the absorption at 420 nm is attributed to the contribution of NQ_{+2H} as the HA product of photo-excited NQ in the absence of oxygen. As shown in Fig. 3, these two absorptions are more and more obvious with the ratio of water increase. Thus, the HA process between ^{3}NQ* and water exists indeed.

Reaction between ^{3}NQ* and adenine in binary water-acetonitrile solutions

Compared with water, the bases prefer to play an efficient role of electron donor due to its lower E_{ox}, instead of hydrogen abstraction. Thus, an electron transfer is expected to occur between ^{3}NQ* and the bases, as shown in Eq. (1).

$$^3NQ^* + \text{base} \rightarrow NQ^{\bullet -} + \text{base}^{\bullet +} \quad (1)$$

Among the bases of G, A, C, T and U, guanine has the lowest E_{ox} value, but it was not studied due to its low solubility in the solvents used. Except for the low E_{ox} value, lone pair electrons of amino nitrogen in $-NH_2$ increase the electron density of the ring and make adenine the easier to lose electrons, thus the electron transfer from A to ^{3}NQ* should be the most feasible.

Figure 4(a) shows the transient absorption spectra of NQ with A (5×10^{-4} M) in an acetonitrile/water solvent of 4:1 volume ratio, while the spectra with A (5×10^{-3} M) are presented in Fig. 4(b). At the same delay time, the spectral intensities of three ^{3}NQ* absorptions are apparently decreased due to quenching by adenine. Three new absorption peaks can be observed with the centers at 343, 420 and 485 nm, besides the absorptions of ^{3}NQ*. In a high concentration of A (5×10^{-3} M), the absorption bands at 374 nm and 660 nm of ^{3}NQ* are almost completely quenched. As the intensities at 343, 420 and 485 nm are increased to the maximums later than the triplet-triplet absorptions of ^{3}NQ*, these bands should come from the absorptions of the reaction products.

It is worth noting that the absorption of $A^{\bullet +}$ is located at ~360 nm (20) and overlapped with that of ^{3}NQ*(T_1) at 374 nm. The overlapping causes the band slightly blueshifted from 374 to

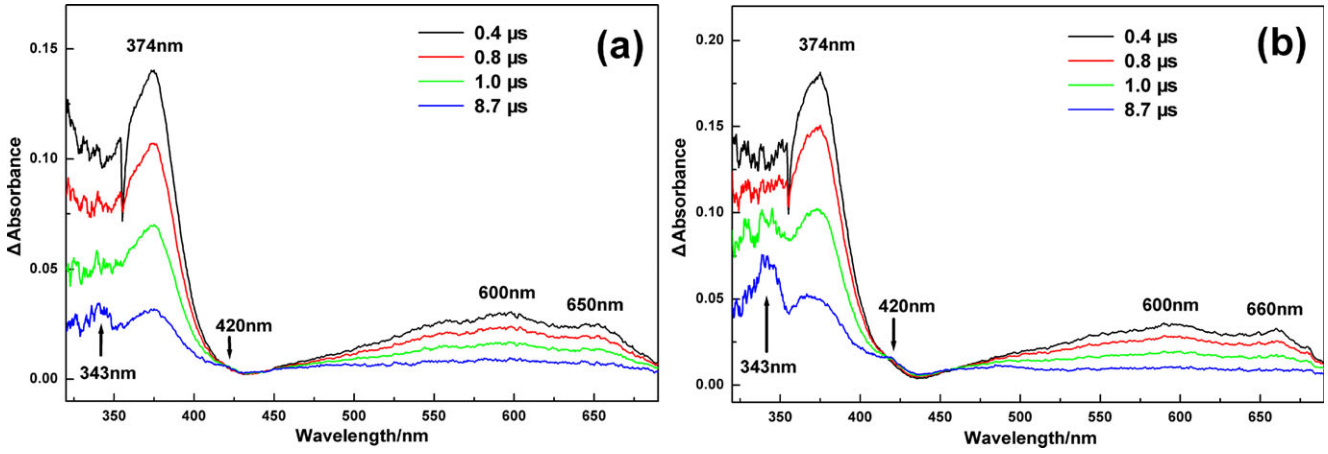

Figure 3. Transient absorption spectra of NQ in (a) CH_3CN/H_2O (9/1, v/v) and (b) CH_3CN/H_2O (4/1, v/v) at different delay times.

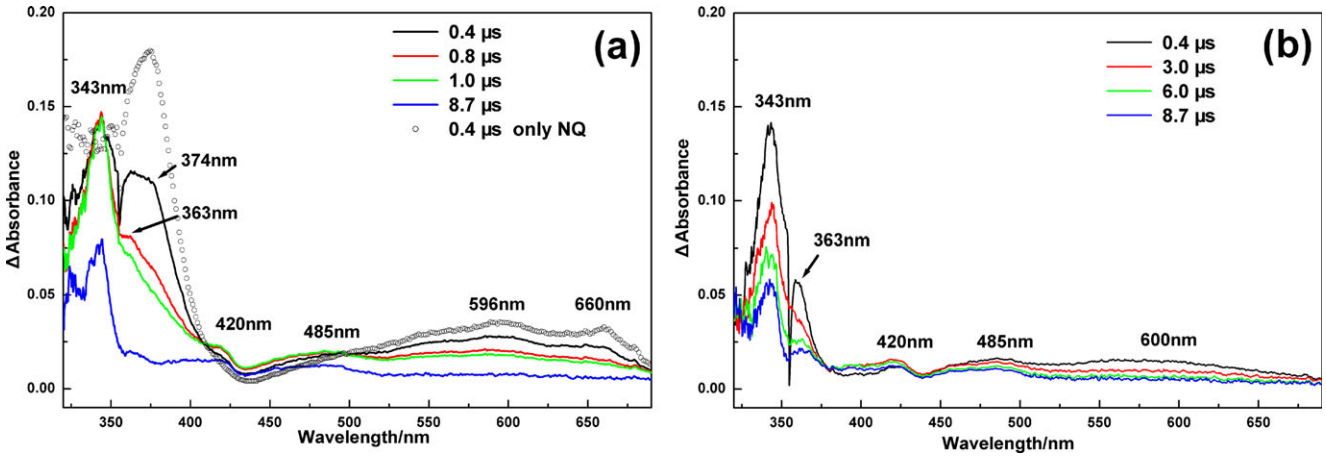

Figure 4. Transient absorption spectra of NQ at different delay times in the presence of A, (a) [A] = 5×10^{-4} M and (b) [A] = 5×10^{-3} M.

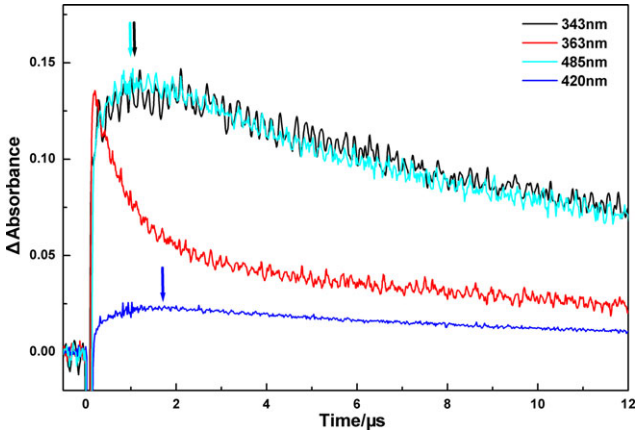

Figure 5. Dynamic decay curves of major absorptions in the reaction system of NQ (5×10^{-4} M) and A (5×10^{-4} M) in the solvent of CH_3CN/H_2O (4/1, v/v).

363 nm in Fig. 4(a). The other product ($NQ^{\bullet -}$) of the electron transfer from A to $^3NQ^*$ cannot be observed due to its absorption that is beyond the wavelength range of the detector (42). As shown in the dynamic decay curves of the major absorptions of Fig. 5, the absorptions at 343 and 485 nm reach the maximums with the almost same rates, and both of them are slower than that at 363 nm, thus the bands are attributed to the products in the secondary reaction between $NQ^{\bullet -}$ and $A^{\bullet +}$. The absorption intensity at 420 nm increases gradually with the slowest rate as expected.

Through fitting the dynamic curves with a bi-exponential function of formula (2), the quenching rates of all the intermediates were obtained and listed in Table 3.

$$I(\lambda) = I_0(\lambda) + A_1(\lambda) \cdot \exp(-k_1 t) + A_2(\lambda) \cdot \exp(-k_2 t) \qquad (2)$$

where $I(\lambda)$ is the absorption intensity at the delay time t, k_1 and k_2 are the faster and slower quenching rates, respectively, $A_1(\lambda)$ and $A_2(\lambda)$ are the weights of both quenching processes, $I_0(\lambda)$-$A_1(\lambda)$-$A_2(\lambda)$ represents the absorption intensity at the initial time. Usually, the faster quenching process is thought as the photochemical reaction, while the slower is the physical quenching (*e.g.* collision).

Compared with that in the absence of A with same solvent, $^3NQ^*$ is efficiently quenched with a much faster quenching rate, indicating that A plays an efficient role of quencher. The initial products are $A^{\bullet +}$ and $NQ^{\bullet -}$. In binary water-acetonitrile solutions, there are three candidates to provide a proton to yield the $NQ_{+H}^{\bullet}$ radical: One is adenine, another is $A^{\bullet +}$ and the other is water. However, the proton transfer from adenine and water is unworkable in thermodynamics, because $H_2O \rightarrow H^+ + OH^-$ and $A \rightarrow A_{-H}^- + H^+$ are very endothermal. In addition, the decay rate of $A^{\bullet +}$ produced from the electron transfer between $^3NQ^*$ and adenine is very fast as shown in Fig. 3, indicating that its quenching is efficient. Due to the strong electrostatic interaction, the proton transfer reaction between $NO^{\bullet -}$ and $A^{\bullet +}$ naturally occurs as Eq. (3). As shown in Fig. 4, the apparent decay rate at 363 nm is reduced to some extent due to the overlap from the absorption of $^3NQ^*$ at 374 nm, and thus we cannot derive the reaction rate directly. The absorption of $NQ_{+H}^{\bullet}$ radical located at 343 nm (35) and its formation process can be directly observed in Fig. 5. The final product, 1,2-

Table 3. Decay rates and absorption wavelengths of intermediates in CH_3CN/H_2O (v/v).

Band	I	II	III	IV	V	VI	VII
NQ +A(5×10^{-4} M) in CH_3CN/H_2O 4/1							
Carrier	$NQ_{+H}^{\bullet}$	$A^{\bullet +}$	$^3NQ^*$	NQ_{+2H}	$NQ_{+H}^{\bullet}$	$^3NQ^*$	$^3NQ^*$
λ (nm)	343	363	374	420	485	596	660
$k(\times 10^6\ s^{-1})$	1.10 ± 0.05	11.23 ± 0.12	15.62 ± 0.04	1.16 ± 0.03	1.12 ± 0.01	14.04 ± 0.14	14.49 ± 0.21
NQ +A(5×10^{-4} M) in CH_3CN/H_2O 9/1							
Carrier	$NQ_{+H}^{\bullet}$	$A^{\bullet +}$	$^3NQ^*$	NQ_{+2H}	$NQ_{+H}^{\bullet}$	$^3NQ^*$	$^3NQ^*$
λ (nm)	343	363	374	420	485	600	660
$k(\times 10^6\ s^{-1})$	1.13 ± 0.05	10.21 ± 0.10	11.91 ± 0.06	1.08 ± 0.03	1.42 ± 0.04	11.49 ± 0.13	12.50 ± 0.16

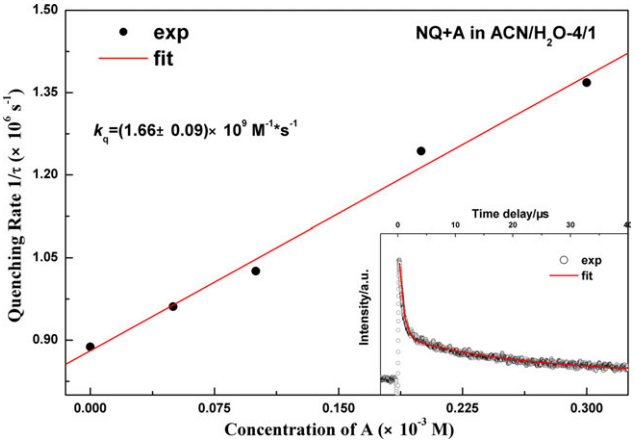

Figure 6. Dependence of the observed quenching rates of ^{3}NQ*on concentration of A in the solvent of CH_3CN/H_2O (4/1, v/v).

dihydroxynaphthalene (NQ_{+2H}), is gradually formed as Eq. (4), and its absorption reaches the maximum at the delay time of ~2 μs in Fig. 5.

$$NQ^{\bullet -} + A^{\bullet +} \rightarrow NQ_{+H}{}^{\bullet} + A_{-H}{}^{\bullet} \quad (3)$$

$$NQ_{+H}{}^{\bullet} + \text{Hydrogen donor} \rightarrow NQ_{+2H} + \text{Product} \quad (4)$$

Moreover, the dynamic behavior of the absorption at 485 nm shows very similar to that at 343 nm in Fig. 5, where the normalized curves at 343 and 485 nm are almost identical with the same decay rates of 1.1×10^6 s^{-1}. Thus, the candidates of the absorption at 485 nm are the $A_{-H}{}^{\bullet}$ radical or another band of the $NQ_{+H}{}^{\bullet}$ radical. An additional experiment was performed to identify the intermediate with absorption at 485 nm. With photolysis at 355 nm, the bands at 343 and 485 nm also exist in the system of NQ and diphenylamine (DPA) in pure acetonitrile. It is well known that an electron transfer occurs between NQ and DPA, and the absorption of $DPA^{\bullet +}$ is located at 780 nm (29). Thus, the band at 485 nm is believed to form by the absorption of $NQ_{+H}{}^{\bullet}$ radical as well as that at 343 nm.

Therefore, a multistep process is confirmed in the reaction between ^{3}NQ* and A: A fast electron transfer is followed by a subsequent proton transfer, and 1,2-dihydroxynaphthalene as the final product is formed via an additional hydrogen abstraction process. Moreover, the quenching rates of ^{3}NQ* are increased with the fraction of water, which is contrary to the case without A in Table 2. Thus, the hydrogen bond looks beneficial to the electron transfer between ^{3}NQ* and A. Through fitting with the Eq. (5) of Stern-Volmer relationship, the quenching rate constant k_q of ^{3}NQ* by A can be determined as 1.66×10^9 M^{-1} s^{-1} as shown in Fig. 6, which is much lower than the theoretical diffusion-controlled rate limit in CH_3CN/H_2O (4/1, v/v) (~ 1.45×10^{10} M^{-1} s^{-1}).

$$1/\tau = 1/\tau_0 + k_q(A) \quad (5)$$

where $1/\tau_0$ and $1/\tau$ are the quenching rate of ^{3}NQ* in solution of the absence and presence of A, respectively. With the ratio of water increase, there is a little bit increase on the quenching rate constant k_q.

Reaction between ^{3}NQ* and T, C and U in binary water-acetonitrile solutions

Figure 7 shows the transient absorption spectra of NQ with T in a solvent of 4:1 volume ratio of acetonitrile/water. Compared with those in the absence of bases (Figs 2 and 3), the spectra look very similar, and no additional peak is observed. All the three ^{3}NQ* absorption bands have a negligible wavelength shift, and two weak bands at 343 and 420 nm are attributed to hydrogen abstraction from water. Because the absorption of the $T^{\bullet +}$ was at 500 nm (18) and no such peak was observed in Fig. 7, the electron transfer did not apparently occur. In addition, the decay rate of ^{3}NQ* at 374 nm is almost the same as that in Fig. 3(b). Thus, we can conclude that no photochemical reaction between NQ and T exists with photolysis at 355 nm. The similar phenomena are also observed for the cases with C and U.

It is well known that the electron transfer can occur when the Gibbs free energy ΔG predicted by the Rehm-Weller Eq. (6) is negative. In general, E_{ox} is the most significant parameter.

$$\Delta G = E_{ox} - E_{red} - q^2/(\varepsilon \cdot r) - E_T \quad (6)$$

where E_{ox} and E_{red} are the oxidation potential of bases and the reduction potential of ^{3}NQ*, respectively, $q^2/(\varepsilon \cdot r)$ is the Coulombic work term of the product ions at the encounter distance r, and E_T is the excited energy of the triplet NQ. The oxidation energies (E_{ox}, *vs* NHE) of the four bases are 1.96 V for A, 2.11 V for T, 2.14 V for C and 2.39 V for U (6), respectively. The reduction potential of ^{3}NQ* is −0.338 V (*vs* NHE) (43). For the ET between the triplet NQ and adenine, the electron is transferred from the amino group, while it is from the ring of pyrimidine for T, C and U. Thus, the effective ET distance in the encounter pair for adenine is smaller than that of pyrimidine and consistent with the calculation of ion pair. Using the calculated values of the encounter distances

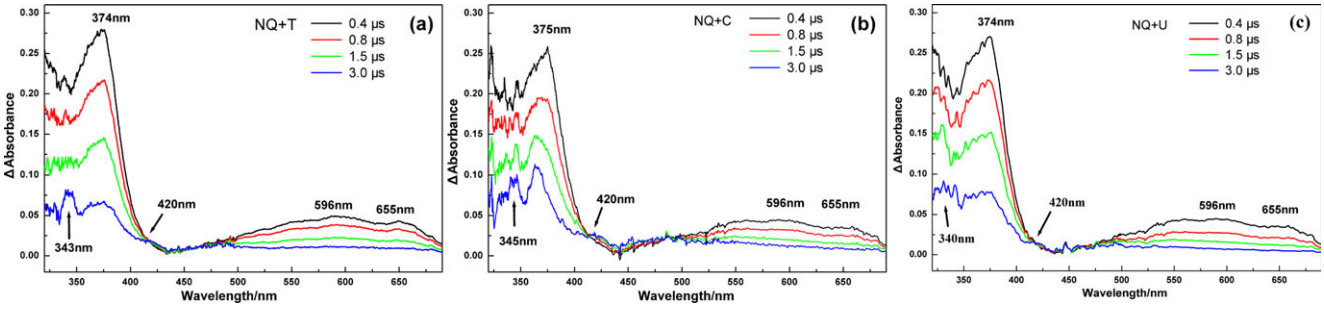

Figure 7. Transient absorption spectra of NQ and three bases at different delay times in CH_3CN/H_2O (4/1, v/v) (a) T, (b) C, (c) U.

between quinone and nucleobases, r(A) = 2.0 Å and r(T/C/U) = 2.5 Å, the Coulombic work is slightly decreased from 3.86 kcal mol^{-1} for A to 3.09 kcal mol^{-1} for T/C/U. The data are larger than the common value, 1.4 kcal mol^{-1} or 0.06 eV, (44) implying that the encounter distances in solutions should be larger than the calculated values. However, the difference of the Coulombic work for the bases can be estimated as 0.77 kcal mol^{-1}, and such small difference suggests that the Coulombic work has very little effect on the total Gibbs free energy. Taking E_T of ^{3}NQ* as 2.11 eV in Table 1, the ΔG values are calculated to be 0.48 kcal mol^{-1} for A, 4.70 kcal mol^{-1} for T, 5.40 kcal mol^{-1} for C and 11.16 kcal mol^{-1} for U, respectively. Thus, the ΔG differences between A and the other three bases are more than 4.22 kcal mol^{-1}, and only ΔG of the reaction between ^{3}NQ* and A is close to zero (or negative) when taking into account the uncertainty. It agrees with the present experimental conclusions. Additionally, the ET possibility sometime does not follow the E_{ox} order in the previous studies, for example, for 1,8-dihydroxyanthraquinone (22) and 9,10-anthraquinone (20), where the steric hindrance plays a significant role as well as E_{ox}. However, the similar phenomena are not observed for the present reaction. Based on the weak dependency of the quenching rate on solvent polarity, the quenching of ^{3}NQ* by adenine more likely takes place along the inner-sphere mechanism.

CONCLUSION

Using nanosecond time-resolved laser flash photolysis, photoreaction between 1,2-NQ and four bases has been investigated. With photo-excitation at 355 nm, the transient absorption spectra of ^{3}NQ* and the other products have been recorded in pure acetonitrile or acetonitrile/water (9/1, 4/1, v/v). All the three bands observed at 374, 596 and 650 nm are attributed to the absorption of the triplet states of NQ. By fitting the decay curve at 374 nm, the relaxation rate of ^{3}NQ* is determined as 8.19×10^6 s^{-1} in pure acetonitrile and slightly decreased with the ratio of water increase. Moreover, two weak absorptions at ~340 and 420 nm are observed in the transient absorption spectra in binary water-acetonitrile solutions, which are assigned as the contributions of the $NQ_{+H}^{\bullet}$ radical (340 nm) and 1,2-dihydroxynaphthalene (NQ_{+2H}, at 420 nm). Thus, a HA process between ^{3}NQ* and water is confirmed.

When adenine exists in solution, a multistep photochemical reaction occurs between ^{3}NQ* and A: The fast electron transfer is followed by the subsequent proton transfer, and 1,2-dihydroxynaphthalene as the final product is formed via an additional hydrogen abstraction process. Besides the absorption bands of ^{3}NQ*, three new bands are observed in the transient spectra at 343, 363 and 485 nm, respectively. The peaks at 343 and 485 nm are both contributed to the $NQ_{+H}^{\bullet}$ radical, while that at 363 nm is attributed to $A^{\bullet+}$. All the spectral assignments agree very well with the previous data or conclusion of the additional experiment of NQ and DPA. By fitting with the Stern-Volmer relationship, the quenching rate constant k_q of ^{3}NQ* by A in binary water-acetonitrile solution (4/1, v/v) is determined as 1.66×10^9 M^{-1} s^{-1}.

In addition, no distinct spectral evidence is obtained for the electron transfer or proton transfer processes between NQ with the other three bases, T, C and U. Thus, ΔG is speculated to change from a negative value for adenine to a positive data for T/C/U. Based on the Rehm-Weller equation, the ΔG values of the electron transfer between ^{3}NQ* and the bases are estimated to increase at least 4.22 kcal mol^{-1} from A to T/C/U.

Acknowledgements—This work was supported by the National Natural Science Foundation of China (No.21373194 and 21573210) and the National Key Basic Research Special Foundation (No.2013CB834602).

SUPPORTING INFORMATION

Additional Supporting Information may be found in the online version of this article:

Figure S1. Steady-state absorption spectra of 1,2-NQ and adenine in pure acetonitrile and binary water-acetonitrile solutions.

Figure S2. Decay curves of ^{3}NQ* at 374 nm in pure acetonitrile in the absence/presence of oxygen.

Figure S3. Transient absorption spectra of NQ in pure acetonitrile at different delay times under photolysis at 450 nm.

Figure S4. Normalized decay curves of ^{3}NQ* at 374, 596 and 650 nm in pure acetonitrile.

REFERENCES

1. Burrows, C. J. and J. G. Muller (1998) Oxidative nucleobase modifications leading to strand scission. *Chem. Rev.* **98**, 1109–1152.
2. Steenken, S. (1989) Purine bases, nucleosides, and nucleotides: aqueous solution redox chemistry and transformation reactions of their radical cations and e- and OH adducts. *Chem. Rev.* **89**, 503–520.
3. Breslin, D. T. and G. B. Schuster (1996) Anthraquinone photonucleases: mechanisms for GG-selective and nonselective cleavage of double-stranded DNA. *J. Am. Chem. Soc.* **118**, 2311–2319.
4. Delatour, T., T. Douki, C. D'Ham and J. Cadet (1998) Photosensitization of thymine nucleobase by benzophenone through energy transfer, hydrogen abstraction and one-electron oxidation. *J. Photochem. Photobiol. B Biol.* **44**, 191–198.
5. Bose, A., A. K. Sarkar and S. Basu (2009) Role of sugar in controlling reaction pathways: a study with thymine and thymidine. *J. Lumin.* **129**, 1186–1191.
6. Seidel, C., A. Schulz and M. H. M. Sauer (1996) Nucleobase-specific quenching of fluorescent dyes. 1. nucleobase one-electron redox potentials and their correlation with static and dynamic quenching efficiencies. *J. Phys. Chem.* **100**, 5541–5553.
7. Chen, J., Y. Huang, G. Liu, Z. Afrasiabi, E. Sinn, S. Padhye and Y. Ma (2004) The cytotoxicity and mechanisms of 1,2-naphthoquinone thiosemicarbazone and its metal derivatives against MCF-7 human breast cancer cells. *Toxicol. Appl. Pharmacol.* **197**, 40–48.
8. Noto, V., H. Taper, Y. Jiang and J. Janssens (1989) Effects of sodium ascorbate (vitamin C) and 2-methyl-1,4-naphthoquinone (vitamin K3) treatment on human tumor cell growth *in vitro*. I. Synergism of combined vitamin C and K3 Action. *Cancer* **63**, 901–906.
9. Thirumurugan, R. S., S. Kavimani and R. S. Srivastava (2000) Antitumour activity of rhinacanthone against dalton's ascitic lymphoma. *Biol. Pharm. Bull.* **23**, 1438–1440.
10. Netto-Ferreira, J. C., V. Lhiaubet-Vallet, B. de Oliveira Bernardes, A. B. B. Ferreira and M. Á. Miranda (2009) Photosensitizing properties of triplet β-lapachones in acetonitrile solution. *Photochem. Photobiol.* **85**, 153–159.
11. Bergeron, F., K. Klarskov, D. J. Hunting and J. R. Wagner (2007) Near-uv photolysis of 2-methyl-1,4-naphthoquinone-DNA duplexes: characterization of reversible and stable interstrand cross-links between quinone and adenine moieties. *Chem. Res. Toxicol.* **20**, 745–756.

12. Ma, J., W. Lin, W. Wang, Z. Han, S. Yao and N. Lin (2000) Triplet state mechanism for electron transfer oxidation of DNA. *J. Photochem. Photobiol. B Biol.* **57**, 76–81.
13. Hartley, J. A., K. Reszka and J. W. Lown (2008) Photosensitization by antitumor agents-7. Correlation between anthracenedione-photosensitized DNA damage, NADH oxidation and oxygen consumption following visible light illumination. *Photochem. Photobiol.* **48**, 19–25.
14. Hayon, E., T. Ibata, N. N. Lichtin and M. Simic (1972) Electron and hydrogen atom attachment to aromatic carbonyl compounds in aqueous solution. Absorption spectra and dissociation constants of ketyl radicals. *J. Phys. Chem.* **76**, 2072–2078.
15. Amada, I., M. Yamaji, M. Sase and H. Shizuka (1995) Laser flash photolysis studies on hydrogen atom abstraction from phenol by triplet naphthoquinones in acetonitrile. *J. Chem. Soc., Faraday Trans.* **91**, 2751–2759.
16. Liu, K., L. Wu, X. Zou, W. Yang, Q. Du and H. Su (2011) Photochemical hydrogen abstraction and electron transfer reactions of tetrachlorobenzoquinone with pyrimidine nucleobases. *Chin. J. Chem. Phys.* **24**, 580–585.
17. Bose, A., D. Dey and S. Basu (2008) Interactions of guanine and guanosine hydrates with quinones: a laser flash photolysis and magnetic field effect study. *J. Phys. Chem. A* **112**, 4914–4920.
18. Bose, A. and S. Basu (2009) Medium-dependent interactions of quinones with cytosine and cytidine: a Laser flash photolysis study with magnetic field effect. *Biophys. Chem.* **140**, 62–68.
19. Bose, A. and S. Basu (2009) Role of sugar in controlling reaction pattern: a comparative study with adenine and 2′-deoxyadenosine. *J. Photochem. Photobiol. A Chem.* **201**, 197–202.
20. Bose, A. and S. Basu (2009) Interaction of quinones with three pyrimidine bases: a laser flash photolysis study. *J. Lumin.* **129**, 1385–1389.
21. Bose, A., D. Dey and S. Basu (2007) Structure-dependent switchover of reaction modes: a laser flash photolysis and magnetic field effect study. *J. Photochem. Photobiol. A Chem.* **186**, 130–134.
22. Liu, X., L. Chen, Q. Zhou, X. Zhou and S. Liu (2013) Electron transfer reactions between 1,8-dihydroxyanthraquinone and pyrimidines: a laser flash photolysis study. *J. Photochem. Photobiol. A Chem.* **269**, 42–48.
23. Murai, H., M. Minami, T. Hayashi and Y. J. I'Haya (1985) Time-resolved ESR study of the lowest excited triplet states of para-quinones in glassy matrices at 77 K. *Chem. Phys.* **93**, 333–338.
24. Murai, H., T. Hayashi and Y. J. I'haya (2017) Time-resolved detection of spin-polarized ESR spectra of 9,10-anthraquinone triplet state in organic glass at 77K. *Chem. Phys. Lett.* **106**, 139–142.
25. Ho, J. H., T. I. Ho, T. H. Chen and Y. L. Chow (2001) Efficient photocycloaddition of phenanthroquinones with simple olefins. *J. Photochem. Photobiol. A Chem.* **138**, 111–122.
26. Zhang, Z., S. Hao, H. Zhu and W. Wang (2008) Photoreactions of 1,4-naphthoquinone with lysozyme studied by laser flash photolysis and steady-state analysis. *J. Photochem. Photobiol. B Biol.* **92**, 77–82.
27. Pan, Y., Y. Fu, S. Liu, H. Yu, Y. Gao, Q. Guo and S. Yu (2006) Studies on photoinduced H-atom and electron transfer reactions of o-naphthoquinones by laser flash photolysis. *J. Phys. Chem. A* **110**, 7316–7322.
28. Tero-kubota, H. S. S. (1989) Influence of solvent polarity on the excited triplet states of nonphosphorescent 1,2-naphthoquinone and phosphorescent 8,l0-phenanthrenequinone: time-resolved triplet ESR and CIDEP Studies. *Society* **93**, 5410–5414.
29. Chen, L., Q. Zhou, X. Liu, X. Zhou and S. Liu (2015) Solvent effect on the photoinduced electron transfer reaction between thioxanthen-9-one and diphenylamine†. *Chin. J. Chem. Phys.* **28**, 493–500.
30. Liu, X., L. Chen, Q. Zhou, X. Zhou and S. Liu (2013) Laser flash photolysis on electron transfer reactions between 1,8-dihydroxyanthraquinone with adenine and cytosine. *Chin. J. Chem. Phys.* **26**, 498–503.
31. Frisch, M. J., G. W. Trucks, H. B. Schlegel, G. E. Scuseria, M. A. Robb, J. R. Cheeseman, G. Scalmani, V. Barone, B. Mennucci and G. A. Petersson (2009) *Gaussian 09*. Gaussian. Inc., Wallingford, CT.
32. Yanai, T., D. P. Tew and N. C. Handy (2004) A new hybrid exchange-correlation functional using the coulomb-attenuating method (CAM-B3LYP). *Chem. Phys. Lett.* **393**, 51–57.
33. Reichardt, C. (2003) *Solvents and Solvent Effects in Organic Chemistry*, 3rd edn. Wiley-VCH Verlag GmbH & Co, KGaA, Weinheim.
34. Bautista, J. A., R. E. Connors, B. B. Raju, R. G. Hiller, F. P. Sharples, D. Gosztola, M. R. Wasielewski and H. A. Frank (1999) Excited state properties of peridinin: observation of a solvent dependence of the lowest excited singlet state lifetime and spectral behavior unique among carotenoids. *J. Phys. Chem. B* **103**, 8751–8758.
35. Harada, Y., S. Watanabe, T. Suzuki and T. Ichimura (2005) Photochemical reaction dynamics of 9,10-phenanthrenequinone and 1,2-naphthoquinone with hydrogen donors in solution. *J. Photochem. Photobiol. A Chem.* **170**, 161–167.
36. Barbafina, A., L. Latterini, B. Carlotti and F. Elisei (2010) Characterization of excited states of quinones and identification of their deactivation pathways. *J. Phys. Chem. A* **114**, 5980–5984.
37. Shi, Y., J. Y. Liu and K. L. Han (2005) Investigation of the internal conversion time of the chlorophyll a from s3, s2 to s1. *Chem. Phys. Lett.* **410**, 260–263.
38. Hamanoue, K., T. Nakayama, M. Shiozaki, Y. Funasaki, K. Nakajima and H. Teranishi (1986) The excited state dynamics of triplet 1,8-dichloroanthraquinone in solutions at room temperature. *J. Chem. Phys.* **85**, 5698–5704.
39. Montalti, M., A. Credi, L. Prodi and M. T. Gandolfi (2006) *Handbook of Photochemistry*, 3rd edn. CRC Press Inc., Boca Raton.
40. Kuhm, A. E., A. Stolz, K. L. Ngai and H. J. Knackmuss (1991) Purification and characterization of a 1,2-dihydroxynaphthalene dioxygenase from a bacterium that degrades naphthalenesulfonic acids. *J. Bacteriol.* **173**, 3795–3802.
41. Maruyama, K., K. Ono and J. Osugi (1972) The photochemical reaction of α-diketones. *Bull. Chem. Soc. Jpn.* **45**, 847–851.
42. Rao, P. S. and E. Hayon (1973) Ionization constants and spectral characteristics of some semiquinone radicals in aqueous solution. *J. Phys. Chem.* **77**, 2274–2276.
43. Meites, L. and P. Zuman (1976) *Handbook Series in Organic Electrochemistry*, Vol. 1. CRC Press Inc., Boca Raton.
44. Faulkner, L. R., H. Tachikawa and A. J. Bard (1972) Electrogenerated chemiluminescence. VII. Influence of an external magnetic field on luminescence intensity. *J. Am. Chem. Soc.* **94**, 691–699.